



# Usefulness of microfocus computed tomography in life science research: preliminary study using murine micro-hepatic tumor models

Takaomi Hagi<sup>1</sup> · Yuji Ishii<sup>2</sup> · Kotaro Yamashita<sup>1</sup> · Takuro Saito<sup>1</sup> · Koji Tanaka<sup>1</sup> · Tomoki Makino<sup>1</sup> · Tsuyoshi Takahashi<sup>1</sup> · Yukinori Kurokawa<sup>1</sup> · Makoto Yamasaki<sup>1</sup> · Hidetoshi Eguchi<sup>1</sup> · Yuichiro Doki<sup>1</sup> · Kiyokazu Nakajima<sup>1,3</sup>

Received: 25 March 2021 / Accepted: 2 August 2021 / Published online: 25 October 2021  
© Springer Nature Singapore Pte Ltd. 2021

## Abstract

**Purpose** Microfocus computed tomography (micro-CT) has not been widely used at high radiation intensity (industrial micro-CT) in life science fields. In this preliminary study, we investigated its potential value in the detection of micro-hepatic tumors in a mouse model.

**Methods** The liver with micro-hepatic tumors was surgically resected en-bloc from mice, and examined with industrial micro-CT and lower intensity micro-CT (small animal micro-CT). The number of hepatic tumors was manually counted on serial images. Then, the accuracy of each technique was determined by preparing matching liver sections and comparing the number of tumors identified in a conventional pathological examination.

**Results** The number of hepatic tumors evaluated with industrial micro-CT showed high concordance with the results of the pathological examinations (intra-class correlation coefficient [ICC]: 0.984; 95% confidence interval [CI] 0.959–0.994). On the other hand, the number of hepatic tumors evaluated with the small animal micro-CT showed low concordance with the number identified in the pathological examinations (ICC: 0.533; 95% CI 0.181–0.815).

**Conclusion** Industrial micro-CT improved the detection of small structures in resected specimens, and might be a promising solution for life science research.

**Keywords** Microfocus computed tomography · Hepatic tumor · Intraoperative diagnosis · Pathological examination

## Introduction

Microfocus computed tomography (micro-CT) is an emerging technique that can provide very high-resolution images of an object by applying a high level of radiation for a long exposure time [1]. This technique (industrial micro-CT) is traditionally used in the engineering industry as a method for testing components nondestructively. It can facilitate the structural analysis of precise machines or important cultural

objects that cannot be damaged [2]. Industrial micro-CT requires long imaging times and the object must maintain its original shape during imaging. Consequently, industrial micro-CT is not currently used as a general technique in life science fields. However, recent studies have demonstrated the feasibility of micro-CT imaging in small animal experiments. In those studies, tumor phenotypes were analyzed with micro-CT, but with restricted radiation levels (small animal micro-CT) [3–6]. In addition, several studies have reported the utility of micro-CT in evaluating ex vivo human tissues, such as lung tumors, breast tumors, and craniopharyngiomas [7–9]. However, few studies have investigated whether micro-CT without restricting the level of radiation is feasible for evaluating resected specimens from digestive organs.

The major goal of the present study was to investigate the utility of industrial micro-CT in a life science field, in particular, for the diagnosis of resected specimens in digestive cancers. However, several appropriate steps should be taken before applying this technique in clinical settings. Therefore,

✉ Kiyokazu Nakajima  
knakajima@gesurg.med.osaka-u.ac.jp

<sup>1</sup> Department of Gastroenterological Surgery, Graduate School of Medicine, Osaka University, Osaka, Japan

<sup>2</sup> CASTEM Co., Ltd., Fukuyama, Japan

<sup>3</sup> Department of Next Generation Endoscopic Intervention (Project ENGINE), Center of Medical Innovation and Translational Research, Osaka University Graduate School of Medicine, Suite 0912, 2-2, Yamadaoka, Suita, Osaka 565-0871, Japan

in this preliminary study, we evaluated the ability of industrial micro-CT to detect hepatic tumors in a mouse model.

## Materials and methods

### Cell lines and animals

Mouse colon adenocarcinoma cells (CT26) were obtained from the American Type Culture Collection (Rockville, MD, USA) and cultivated in RPMI-1640 medium (Life Technologies, Carlsbad, CA, USA) supplemented with 10% fetal bovine serum (Sigma-Aldrich, St. Louis, MO, USA) and antibiotics. Cultures were maintained at 37 °C in a humidified atmosphere containing 5% CO<sub>2</sub>. An 8-week-old male BALB/c mice were purchased from CLEA Japan (Tokyo, Japan). Mice were maintained in a temperature-controlled room (24 °C) and under specific pathogen-free conditions. All experiments were conducted according to the Institutional Ethical Guidelines for Animal Experimentation of Osaka University (no. 30-028-004).

### Experimental hepatic tumor model

To create the experimental hepatic tumor model, the spleen was exposed with a 5-mm incision in the left hypochondrium [10]. Next, an inoculation of  $2.0 \times 10^6$  CT26 cells in 100 µL phosphate-buffered saline was injected into the inferior pole of the spleen. One minute later, the splenic vessels were ligated, and the mouse was splenectomized. Fourteen days after the injection, 100 µL of a contrast agent for small animals (ExiTron nano 6000; Miltenyi Biotec, Bergisch-Gladbach, Germany) was injected into the tail vein. At 24 h after injecting the contrast agent, the liver was harvested en bloc and fixed with 4% paraformaldehyde. All procedures were performed under anesthesia with isoflurane.

### Micro-CT imaging

Images of the paraformaldehyde-fixed mouse liver were acquired twice. The first acquisition was performed with an MCT225 micro-CT scanner (Nikon Instech Co., Ltd., Tokyo, Japan), which is commonly used for industrial applications (industrial micro-CT). The second acquisition was performed with an R\_mCT2 micro-CT scanner (Rigaku Corporation, Tokyo, Japan), which is commonly used in small animal experiments with restricted levels of radiation (small animal micro-CT).

Imaging with the MCT225 micro-CT scanner (industrial micro-CT) was performed at an X-ray setting of 90 kV, 90 µA, and 8.1 W, with a 100-µm aluminum filter. The X-ray source detector pair was fixed, with a 3-µm focal spot size. The fixed liver, in a plastic container, was

placed on a rotating table, at a distance of 1 cm from the X-ray source (Fig. 1A, B). The liver was rotated through 360° and received a 1.415-s exposure at each 0.129° increment. In addition, at each angle, the image was acquired twice to reduce scanning noise. The total exposure time was 132 min. Image reconstruction was performed with VG Studio MAX (Volume Graphics GmbH, Heidelberg, Deutschland), with standard filtered back projection and a 14-µm square voxel size (i.e., slice thickness of coronal sectioned images). Three-dimensional images were constructed with a semi-automated image processing software program (IMARIS; Bitplane AG, Zurich, Switzerland).

Imaging with the R\_mCT2 micro-CT scanner (small animal micro-CT) was performed at 90 kV, 160 µA, and 14.4 W, with a 30-µm square voxel size. This CT scanner was a cone-beam type with a 5-µm X-ray focal spot size. The X-ray source-detector pair rotated around the fixed liver, which was placed on a central platform, and the liver received 0.352 s of exposure at each 0.703° increment. The total exposure time was 3 min (Fig. 1C).

The detection of tumors was defined as lesions that were not contrasted by the agent and which had clear borders. In addition, among those that were not contrasted, the lesions that could be traced on consecutive slices were considered as vessels in the liver. The detection of the tumors was evaluated by an investigator (T.H.).

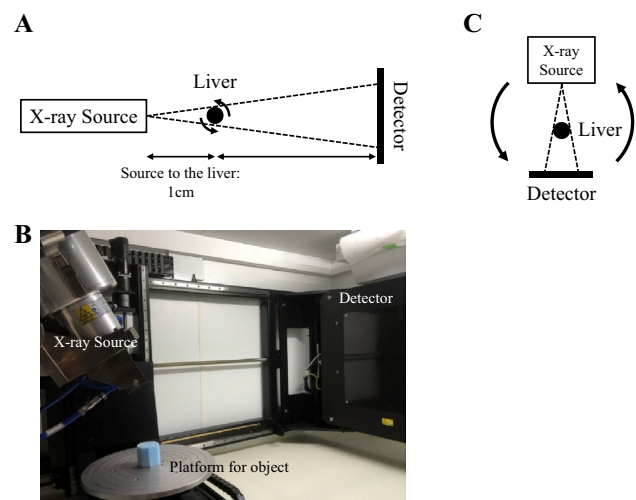


**Fig. 1** Structural designs of micro-CT scanners. **A** A schematic illustration and **B** the inside of an industrial micro-CT scanner. The object on the platform rotates 360° for imaging. The distance between the X-ray source and the object is adjustable, and it regulates the resolution of the image. In our study, the liver was placed 1 cm from the X-ray source. **B** A schematic illustration of a small animal micro-CT scanner. The design of the small animal micro-CT is similar to that of a medical CT scanner

## Pathological examination

After the completion of the micro-CT imaging procedures, the specimen was embedded in paraffin. Then, the specimen was cut into 4- $\mu$ m thick sections, parallel to the coronal axis. We prepared pathological sections of the liver that matched the two types of micro-CT images, at every 1 mm. Sections were stained with hematoxylin and eosin for microscopic examination. The number of tumors in the liver with a diameter of 100- $\mu$ m or more was counted on every 1-mm section by an investigator (T.H.), with a BZ-X710 microscope equipped with the Hybrid Cell Count software program (KEYENCE, Itasca, IL, USA).

## Statistical analysis

A number of tumors counted with each micro-CT device were compared with the numbers counted in pathological examinations of 20 sections. Agreement was evaluated with the intraclass correlation coefficient (ICC) and 95% confidence interval (95% CI). All statistical analyses were performed with the SPSS software program (version 22.0; IBM Corp., Armonk, NY, USA).

## Results

### Evaluation of hepatic tumors with industrial micro-CT

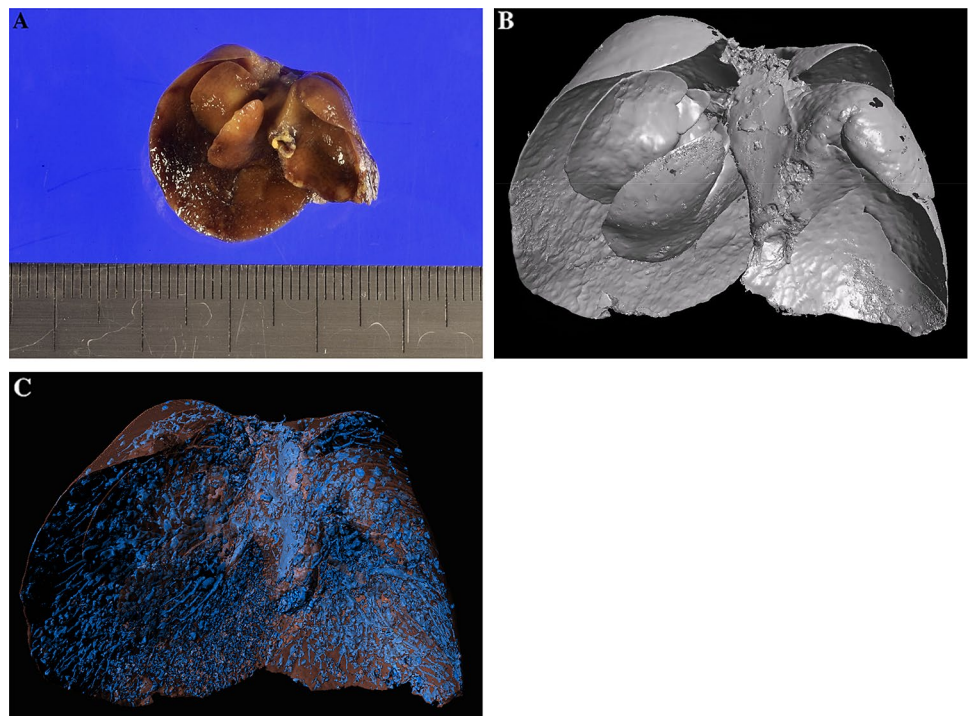
The resected mouse liver was 26  $\times$  23  $\times$  20 mm (Fig. 2A). We created a three-dimensional reconstruction of the surface of the liver, using industrial micro-CT data (Fig. 2B and Additional file 1: Video 1). In addition, we created a three-dimensional reconstruction that focused on the tumors and vessels of the liver, using industrial micro-CT data (Fig. 2C), to examine the detailed structures of the tumors and vessels in the liver. The isotropic voxel size was 14  $\mu$ m.

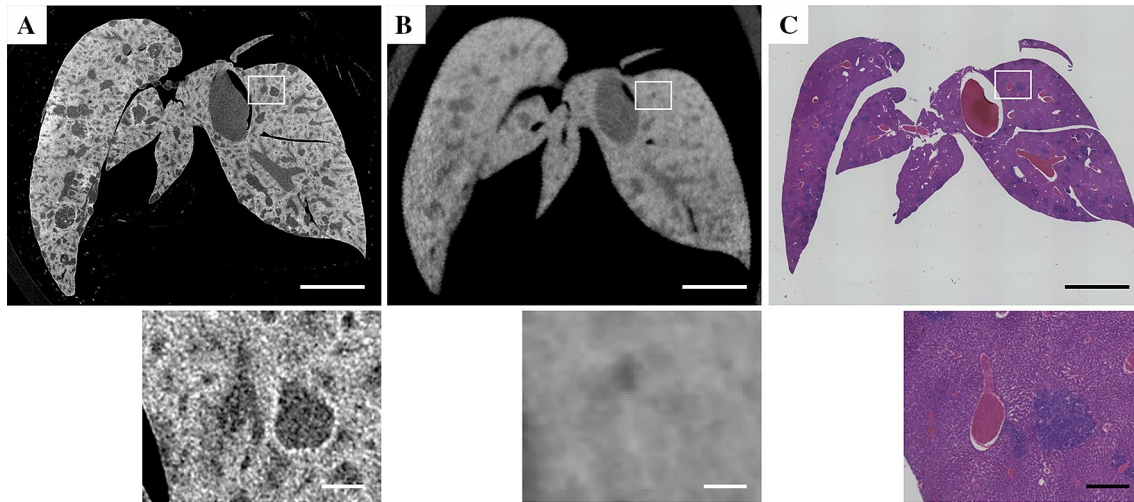
### Comparison between two micro-CT approaches and the pathological examination

Figure 3 shows micro-CT images of the resected liver sections, acquired by the two types of micro-CT devices. These sections were matched to pathological sections stained with hematoxylin and eosin.

Figure 4 shows the analysis of the number of hepatic tumors detected with each micro-CT device, which was compared with the number identified in the pathological examination. The number of hepatic tumors evaluated with industrial micro-CT was highly concordant with the number identified in the pathological examination (ICC: 0.984; 95% CI 0.959–0.994). On the other hand, the number of hepatic

**Fig. 2** Images of the resected mouse liver acquired by industrial micro-CT. **A** Macroscopic examination of the resected mouse liver. Tumors were identified at the surface of the liver. **B, C** Three-dimensional reconstruction images of **B** the surface and **C** the inside the liver, based on the industrial micro-CT data. Blue indicates the border of the tumors and the vessels of the liver. Brown indicates the surface of the liver





**Fig. 3** Comparison of different micro-CT imaging techniques for evaluating a section of resected mouse liver. Images of a single mouse liver section acquired by **A** industrial micro-CT or **B** small animal micro-CT were compared with **C** a micrograph of the same

section from a pathological examination. Insets at the bottom of each image show the area within the small rectangle at higher magnification. Scale bars at lower magnification indicate 5000  $\mu\text{m}$ ; scale bars at higher magnification indicate 500  $\mu\text{m}$

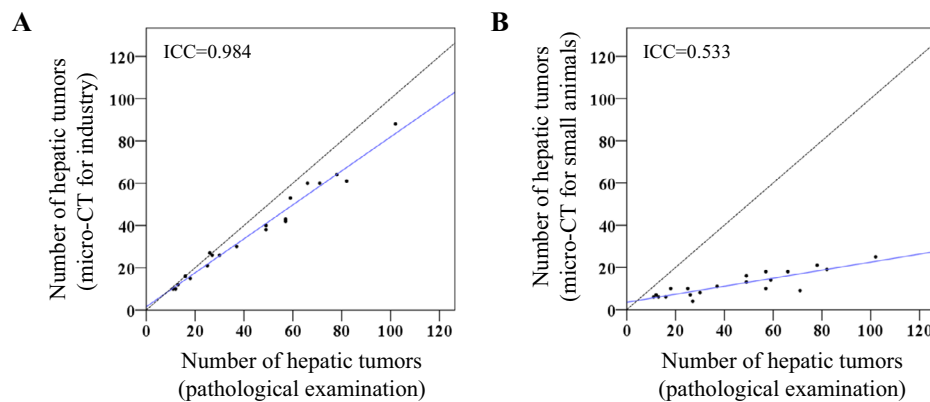


**Fig. 4** Analysis of the number of hepatic tumors identified with micro-CT. The number of tumors identified with **A** industrial micro-CT and **B** small animal micro-CT is compared with the number identified in the pathological examination. The number of hepatic tumors evaluated by industrial micro-CT was highly concordant with the

number identified in the pathological examination, while small animal micro-CT showed low concordance. Black dotted lines are reference lines, which indicate where the vertical value = horizontal value. Blue lines indicate approximate lines. *ICC* intraclass correlation coefficient

tumors evaluated with the small animal micro-CT showed low concordance with the number identified in the pathological examination (*ICC*: 0.533; 95% *CI* 0.181–0.815).

## Discussion

The micro-CT technique has been used extensively in small animal experiments; however, the level of radiation applied was restricted. In human samples, such as surgically resected tissues, only a few studies have used micro-CT without restricting the level of radiation applied; those studies were mostly focused on breast tissues [9, 11]. Tang et al. reported

the utility of micro-CT in assessing a shaved cavity margin and in determining the accurate size of a tumor in resected breast cancer specimens [12, 13]. McClatchy et al. rapidly assessed surgical margins with micro-CT during breast-conserving surgery. They also investigated the correlation between micro-CT findings and the final histopathological findings [11].

In this study, we investigated the utility of industrial micro-CT in detecting micro-tumors in a mouse model. Micro-tumors are difficult to identify macroscopically in the mouse liver. We found that the number of hepatic tumors evaluated with industrial micro-CT was highly concordant with the number identified in the pathological examination,

while small animal micro-CT showed low concordance. Although some issues remain to be resolved, this technique may improve the detection of small structures in resected specimens.

Nevertheless, the micro-CT technique has not been used widely in life science fields, because it is very difficult to image soft tissues. First, micro-CT requires a long time to image an object. During that imaging time, soft tissues often undergo subtle changes in shape, due to the effects of gravity and respiration. These movements lead to a blurry image or artifacts. In previous studies, breast cancer specimens were compressed between two acrylic plates, which fixed the shape during imaging. In our study, the liver was fixed in a plastic container to avoid subtle changes in shape.

Second, tumor identification is difficult, because the contrast is poor between normal liver tissues and tumors and between the liver and other organs. Therefore, identifying a tumor or examining intrahepatic construction is troublesome without a contrast agent. In this study, we used a hepatocyte-selective contrast agent for imaging. This contrast agent is an alkaline, earth-based nanoparticle, which is taken up by cells of the reticuloendothelial system, including Kupffer cells within the liver [14]. However, this contrast agent is only designed for preclinical CT imaging, and it cannot be administered to human subjects. To ensure micro-CT is relevant to clinical practice, it is necessary to consider either using other contrast agents, which are currently approved, or not administering a contrast agent. Alternatively, the specimens can be incubated with contrast agents after resection. For example, gadolinium ethoxybenzyl diethylenetriaminepentaacetic acid is a hepatobiliary contrast agent that is widely used in magnetic resonance imaging (MRI) to diagnose hepatic tumors [15, 16]. Mi et al. reported a pH-activatable nanoparticle contrast agent that could identify small hepatic tumors in MRIs [17]. De Gooyer et al. recently reported that colorectal cancer tumors could be detected in resected specimens placed in tissue culture medium containing a carcinoembryonic antigen-targeting tracer [18]. Combining these agents with micro-CT imaging might provide better detection of tumor tissues, and thereby, improve the diagnosis. In the future, the development of a new contrast agent is expected.

In the recent years, imaging devices and imaging analysis software programs have been developing rapidly. In the field of CT imaging, nano-CT, which provides much higher resolution than current micro-CT, is now becoming widely adopted [19–21]. The advances in this field might reduce the cost of devices, which could lead to the widespread use of micro-CT. In turn, the widespread adoption of this technique might expand its use to diagnostic, treatment, and education settings. Taking full advantage of this new technique might revolutionize life science research.

The present study was associated with several limitations. First, industrial micro-CT imaging required a long exposure

time, which is not ideal for evaluations during surgery. The long exposure times were necessary, because the micro-CT device we used was designed to target large samples, up to 450 mm in diameter. However, other micro-CT devices are designed to target smaller samples, which could shorten the imaging time. Future studies should be conducted with optimal devices. Second, our contrast agent only enhanced hepatocytes; therefore, hepatic tumors and vessels were difficult to distinguish from each other. Furthermore, we could not classify these structures with different colors in three-dimensional reconstruction images (Fig. 2C). Therefore, we evaluated the number of hepatic tumors by confirming the identified tumors and vessels on consecutive images. Third, the individually matched liver section images may have been slightly misaligned by the modalities. Although we attempted to adjust the axis of each image to suit all modalities, subtle misalignments occurred, which may have affected the counts of hepatic tumors. These limitations should be considered in future studies.

In conclusion, this preliminary study demonstrated the potential utility of industrial micro-CT in the diagnostic evaluation of resected liver specimens. We showed that the high resolution of industrial micro-CT could facilitate the identification of hepatic micro-tumors in a mouse model. Although several problems must be resolved before industrial micro-CT can be used in clinical applications, the present study showed that this novel modality might be useful as a diagnostic aid in surgical treatment. In the future, a prospective clinical study should be undertaken to investigate whether this technique can facilitate the quantification of liver tumors.

**Supplementary Information** The online version contains supplementary material available at <https://doi.org/10.1007/s00595-021-02396-1>.

**Funding** The authors declare that this study received no funding.

## Declarations

**Conflicts of interest** The authors declare no conflicts of interest in association with the present study.

## References

1. Hutchinson JC, Shelmerdine SC, Simcock IC, Sebire NJ, Arthurs OJ. Early clinical applications for imaging at microscopic detail: microfocus computed tomography (micro-CT). *Br J Radiol*. 2017;90:20170113.
2. Freeth T, Bitsakis Y, Moussas X, Seiradakis JH, Tselikas A, Mangou H, et al. Decoding the ancient Greek astronomical calculator known as the antikythera mechanism. *Nature*. 2006;444:587–91.
3. Montet X, Pastor CM, Vallée JP, Becker CD, Geissbuhler A, Morel DR, et al. Improved visualization of vessels and hepatic tumors by micro-computed tomography (CT) using iodinated liposomes. *Invest Radiol*. 2007;42:652–8.

4. Almajdub M, Nejari M, Poncet G, Magnier L, Chereul E, Roche C, et al. In-vivo high-resolution X-ray microtomography for liver and spleen tumor assessment in mice. *Contrast Media Mol Imaging*. 2007;2:88–93.
5. Haines BB, Bettano KA, Chenard M, Sevilla RS, Ware C, Angagaw MH, et al. A quantitative volumetric micro-computed tomography method to analyze lung tumors in genetically engineered mouse models. *Neoplasia*. 2009;11:39–47.
6. Badea CT, Panetta D. High-resolution CT for small-animal imaging research. *Compr Biomed Phys*. 2014;2:221–42.
7. Scott AE, Vasilescu DM, Seal KA, Keyes SD, Mavrogordato MN, Hogg JC, et al. Three dimensional imaging of paraffin embedded human lung tissue samples by micro-computed tomography. *PLoS ONE*. 2015;10:e0126230.
8. Apps JR, Hutchinson JC, Arthurs OJ, Virasami A, Joshi A, Zeller-Plumhoff B, et al. Imaging Invasion: micro-CT imaging of adamantinomatous craniopharyngioma highlights cell type specific spatial relationships of tissue invasion. *Acta Neuropathol Commun*. 2016;4:57.
9. Tang R, Buckley JM, Fernandez L, Coopey S, Aftreth O, Michaelson J, et al. Micro-computed tomography (Micro-CT): a novel approach for intraoperative breast cancer specimen imaging. *Breast Cancer Res Treat*. 2013;139:311–6.
10. Hagi T, Kurokawa Y, Kobayashi N, Takahashi T, Saito T, Yamashita K, et al. Anti-metastatic effect of methylprednisolone targeting vascular endothelial cells under surgical stress. *Sci Rep*. 2021. <https://doi.org/10.1038/s41598-021-85241-2>.
11. McClatchy DM 3rd, Zuurbier RA, Wells WA, Paulsen KD, Pogue BW. Micro-computed tomography enables rapid surgical margin assessment during breast conserving surgery (BCS): correlation of whole BCS micro-CT readings to final histopathology. *Breast Cancer Res Treat*. 2018;172:587–95.
12. Tang R, Coopey SB, Buckley JM, Aftreth OP, Fernandez LJ, Brachtel EF, et al. A pilot study evaluating shaved cavity margins with micro-computed tomography: a novel method for predicting lumpectomy margin status intraoperatively. *Breast J*. 2013;19:485–9.
13. Tang R, Saksena M, Coopey SB, Fernandez L, Buckley JM, Lei L, et al. Intraoperative micro-computed tomography (micro-CT): a novel method for determination of primary tumour dimensions in breast cancer specimens. *Br J Radiol*. 2016;89:20150581.
14. Boll H, Nittka S, Doyon F, Neumaier M, Marx A, Kramer M, et al. Micro-CT based experimental liver imaging using a nanoparticulate contrast agent: a longitudinal study in mice. *PLoS ONE*. 2011;6:e25692.
15. Reimer P, Rummeny EJ, Shamsi K, Balzer T, Daldrup HE, Tombach B, et al. Phase II clinical evaluation of Gd-EOB-DTPA: dose, safety aspects, and pulse sequence. *Radiology*. 1996;199:177–83.
16. Hamm B, Staks T, Mühler A, Bollow M, Taupitz M, Frenzel T, et al. Phase I clinical evaluation of Gd-EOB-DTPA as a hepatobiliary MR contrast agent: safety, pharmacokinetics, and MR imaging. *Radiology*. 1995;195:785–92.
17. Mi P, Kokuryo D, Cabral H, Wu H, Terada Y, Saga T, et al. A pH-activatable nanoparticle with signal amplification capabilities for non-invasive imaging of tumour malignancy. *Nat Nanotechnol*. 2016;11:724–30.
18. de Gooyer JM, Elekonawo FMK, Bos DL, van der Post RS, Pèlegriin A, Framery B, et al. Multimodal CEA-targeted image-guided colorectal cancer surgery using <sup>111</sup>In-labeled SGM-101. *Clin Cancer Res*. 2020. <https://doi.org/10.1158/1078-0432.CCR-20-2255> (**Online ahead of print**).
19. Takeuchi A, Suzuki Y. Recent progress in synchrotron radiation 3D–4D nano-imaging based on X-ray full-field microscopy. *Microscopy (Oxf)*. 2020. <https://doi.org/10.1093/jmicro/dfaa022> (**Online ahead of print**).
20. Santos de Oliveira C, González AT, Hedtke T, Kürbitz T, Heilmann A, Schmelzer CEH, et al. Direct three-dimensional imaging for morphological analysis of electrospun fibers with laboratory-based Zernike X-ray phase-contrast computed tomography. *Mater Sci Eng C Mater Biol Appl*. 2020;115:111045.
21. Ditscherlein R, Furat O, de Langlard M, Martins de Souza E Silva J, Sygusch J, Rudolph M, et al. Multiscale tomographic analysis for micron-sized particulate samples. *Microsc Microanal*. 2020;26:676–88.

**Publisher's Note** Springer Nature remains neutral with regard to jurisdictional claims in published maps and institutional affiliations.